Proceedings of the 1996 IEEE
International Conference on Robotics and Automation
Minneapolis, Minnesota - April 1996

Optimization of the Inertial and Acceleration Characteristics of Manipulators

Oussama Khatib and Alan Bowling
Robotics Laboratory
Department of Computer Science
Stanford University, Stanford, CA 94086

Abstract

This article investigates the problem of manipulator design for increased dynamic performance. Optimization techniques are used to determine the design parameters which improve manipulator performance. The dynamic performance of a manipulator is characterized by the inertial and acceleration properties of the end-effector. Our study of inertial and acceleration properties have provided separate descriptions of the characteristics associated with linear and angular motions. This allows a more physically meaningful interpretation of these properties and provides simple models for their analysis. The article presents these models, discusses the design optimization criteria, and formulates the optimization problem. The approach is illustrated in the selection of design parameters of a parallel mechanism.

1 Introduction

The initial design of a manipulator is often based on considerations dealing with its kinematic structure and workspace. This initial design must then be analyzed to examine its dynamic performance. A manipulator dynamic performance involves issues dealing with how quickly the system responds to actuator commands and how it reacts to contact forces and moments. These concerns translate into the study of the end-effector acceleration and inertial characteristics.

A number of studies has addressed the characterization of inertial and acceleration properties of manipulators. The inertial properties have been explored using the generalized inertia ellipsoid [1], the ellipsoid of gyration [3], and the belted inertia ellipsoid [4]. The proposed measures of acceleration capability include the dynamic manipulability [10], the acceleration parallelepiped [5], the acceleration sets [7], and the ellipsoid expansion model [2].

Modifying a manipulator's design parameters can improve the end-effector inertial and acceleration characteristics thereby improving dynamic performance. Our previous work in this area, [5] and [6], resulted in a methodology for optimizing the dynamic performance of manipulators.

These studies have also revealed the difficulty of dealing with the non-homogeneity issues between properties governing linear and angular motions. Typically, these issues are handled by introducing scaling factors to compensate for the differences between properties affecting linear and angular motions. In practice, these scaling factors can be somewhat arbitrary and difficult to determine. The work presented here resolves these issues using new characterizations of inertial and acceleration characteristics in the formulation of the optimization problem.

We have recently presented a characterization that provides a decomposition of the inertial properties into *effective mass* and *effective inertia* associated with the end-effector's linear and angular motions [4]. The ellipsoid expansion model [2] we have proposed for the description the acceleration capability also provides separate measures for linear and angular acceleration. These models are the basis for the formulation presented in this article.

The goal of the optimization is to obtain a design with the smallest, most isotropic inertial characteristics, and the largest, most isotropic acceleration capability at the end-effector over the workspace. First we present the models for the characterization of the inertial and acceleration properties. These models will be extended for redundant manipulators. We will then discuss the optimization scheme and cost function. Results from the application of this scheme to the design of a parallel mechanism will be presented.

2 Inertial Properties

The joint space equations of motion of a manipulator are

$$A(\mathbf{q})\ddot{\mathbf{q}} + \mathbf{b}(\dot{\mathbf{q}}, \mathbf{q}) + \mathbf{g}(\mathbf{q}) = \tau, \qquad (1)$$

where $\mathbf{q}$ is the vector of n joint coordinates, $A(\mathbf{q})$ is

the joint space kinetic energy matrix, $\mathbf{b}(\dot{\mathbf{q}}, \mathbf{q})$ is the vector of centrifugal and Coriolis forces, $\mathbf{g}(\mathbf{q})$ is the gravity vector, and τ is the vector of joint torques.

For a redundant manipulator, the dynamic behavior at the end-effector is described by the equation [4]

$$\Lambda(\mathbf{q})\dot{\vartheta} + \mu(\mathbf{q}, \dot{\mathbf{q}}) + \mathbf{p}(\mathbf{q}) = \mathbf{F}; \tag{2}$$

where $\Lambda(\mathbf{q})$ is the pseudo kinetic energy matrix

$$\Lambda^{-1}(\mathbf{q}) = J(\mathbf{q})A^{-1}(\mathbf{q})J^T(\mathbf{q}) \tag{3}$$

and $\mu(\mathbf{q}, \dot{\mathbf{q}})$, $\mathbf{p}(\mathbf{q})$, and $\mathbf{F}$ are respectively the centrifugal and Coriolis force vector, gravity force vector, and generalized force vector acting in operational space. ϑ along with the Jacobian matrix [4], $J(\mathbf{q})$, are defined as

$$\vartheta \triangleq \begin{bmatrix} v \\ \omega \end{bmatrix} = J(\mathbf{q})\dot{\mathbf{q}}. \tag{4}$$

where v and ω are the end-effector linear and angular velocities.

The relationship between joint torques and operational forces for redundant manipulator is

$$\tau = J^T(\mathbf{q})\mathbf{F} + \left[I - J^T(\mathbf{q})\overline{J}^T(\mathbf{q})\right]\tau_0; \tag{5}$$

where τ_0 is an arbitrary joint torque vector, and

$$\bar{J}(\mathbf{q}) = A^{-1}(\mathbf{q})\ J^T(\mathbf{q})\ \Lambda(\mathbf{q}). \tag{6}$$

The matrix $\bar{J}(\mathbf{q})$ is the *dynamically consistent generalized inverse* of the Jacobian matrix $J(\mathbf{q})$, and I is the identity matrix.

This relationship of equation (5) provides a decomposition of joint forces into two dynamically decoupled control vectors: joint forces corresponding to forces acting at the end effector $(J^T(\mathbf{q})\mathbf{F})$; and joint forces that only affect internal motions, $\left([I - J^T(\mathbf{q})\overline{J}^T(\mathbf{q})]\tau_0\right)$.

$\Lambda(\mathbf{q})$ describes the inertial properties as perceived at the end-effector. The eigenvalues and eigenvectors of $\Lambda(\mathbf{q})$ usually represent some mixture of mass and inertia properties. However, the analysis of the matrix $\Lambda(\mathbf{q})$ reveals a structure that allows separate characterization of the inertial properties for linear and angular motion [4]. The analysis is based on a decomposition of the Jacobian matrix into its linear and angular sub-matrices:

$$J(\mathbf{q}) = \begin{bmatrix} J_v(\mathbf{q}) \\ J_\omega(\mathbf{q}) \end{bmatrix} \tag{7}$$

where the matrix $J_v(\mathbf{q})$ transforms joint velocities into end-effector linear velocities and $J_\omega(\mathbf{q})$ does likewise for end-effector angular velocities. The kinematic structure of the particular manipulator will determine the dimensions or existence of $J_v(\mathbf{q})$ and $J_\omega(\mathbf{q})$. Using equation (7) the the matrix $\Lambda^{-1}(\mathbf{q})$ can be written in the form

$$\Lambda^{-1}(\mathbf{q}) = \begin{bmatrix} \Lambda_v^{-1}(\mathbf{q}) & \overline{\Lambda}_{v\omega}(\mathbf{q}) \\ \overline{\Lambda}_{v\omega}^T(\mathbf{q}) & \Lambda_\omega^{-1}(\mathbf{q}) \end{bmatrix}, \tag{8}$$

where $\Lambda_v(\mathbf{q})$ is

$$\Lambda_v = (J_v(\mathbf{q})A^{-1}(\mathbf{q})J_v^T(\mathbf{q}))^{-1} \tag{9}$$

and

$$\Lambda_\omega = (J_\omega(\mathbf{q})A^{-1}(\mathbf{q})J_\omega^T(\mathbf{q}))^{-1}. \tag{10}$$

The matrix $\overline{\Lambda}_{v\omega}(\mathbf{q})$ is given by

$$\overline{\Lambda}_{v\omega}(\mathbf{q}) = J_v(\mathbf{q})A^{-1}(\mathbf{q})J_\omega^T(\mathbf{q}).$$

The matrix $\Lambda_v(\mathbf{q})$, which describes the end-effector translational response to a force, is homogeneous to a mass matrix, while $\Lambda_\omega(\mathbf{q})$, which describes the end-effector rotational response to a moment, is homogeneous to an inertia matrix. The matrix $\overline{\Lambda}_{v\omega}(\mathbf{q})$ provides a description of the coupling between translational and rotational motions.

As stated earlier, part of the goal in the optimization is to achieve the smallest, most isotropic inertial properties. The magnitude of these properties is described by the norm of Λ_v and Λ_ω, $\|\Lambda_v\|$ and $\|\Lambda_\omega\|$. The condition numbers of the two matrices, $\kappa(\Lambda_v)$ and $\kappa(\Lambda_\omega)$, describes the extent of isotropicity of the inertial properties. These indicators will be used in the cost function in our optimization.

3 Acceleration Characteristics:

The ellipsoid expansion model provides a simple framework for analyzing end-effector acceleration capability. In this model acceleration capability is characterized by the isotropic acceleration, defined as the maximum acceleration achievable in or about every direction. In the development of this model we consider the bounds on joint torques which are determined by the maximum torque of the actuators,

$$-\tau_{bound} \leq \tau \leq \tau_{bound}. \tag{11}$$

The joint torque, τ, consists of torques required to compensate for gravity and torques required to produce end-effector motion,

$$J^T(\Lambda\dot{\vartheta} + \mu) + \mathbf{g} = \tau. \tag{12}$$

Analysis of other requirements, such as the performance of motions in the null space, can be easily integrated into this formulation.

The bounds are normalized using a diagonal matrix N with elements $N_{ii} = \frac{1}{\tau_{bound_i}}$. Now using equations (12) and (11) yields,

$$-\mathbf{1} \leq NJ^T(\Lambda\dot{\vartheta} + \mu) + N\mathbf{g} \leq \mathbf{1}; \quad (13)$$

where $\mathbf{1}$ is a vector of dimension n with each element equal to one. Using equation (6) the above equation can be rewritten as,

$$\tau_{lower} \leq [E_v \; E_\omega] \begin{bmatrix} \dot{v} \\ \dot{\omega} \end{bmatrix} + \begin{bmatrix} \vartheta^T M_1 \vartheta \\ \vdots \\ \vartheta^T M_n \vartheta \end{bmatrix} \leq \tau_{upper}; \quad (14)$$

where M_i are symmetric matrices and,

$$[E_v \; E_\omega] = NJ^T\Lambda; \quad (15)$$

$$\begin{bmatrix} \vartheta^T M_1 \vartheta \\ \vdots \\ \vartheta^T M_n \vartheta \end{bmatrix} = NJ^T\mu; \quad (16)$$

$$\tau_{upper} = \mathbf{1} - N\mathbf{g}; \quad (17)$$

$$\tau_{lower} = -\mathbf{1} - N\mathbf{g}. \quad (18)$$

The central equation for this analysis is

$$\tau_{lower} \leq E_v\dot{v} + E_\omega\dot{\omega} + \begin{bmatrix} \vartheta^T M_1 \vartheta \\ \vdots \\ \vartheta^T M_n \vartheta \end{bmatrix} \leq \tau_{upper} \quad (19)$$

The separation of linear and angular accelerations in equation (19) is motivated by the need to analyze each of them independently.

As stated earlier, the aim in this optimization is to achieve the largest, most isotropic end-effector acceleration capability. The extent of the magnitude and isotropicity of the acceleration capability will be measured by the norm and condition numbers of the matrices E_v and E_ω which will be used in our cost function.

3.1 Analysis

In the ellipsoid expansion model, the end-effector acceleration capability is analyzed by determining the end-effector isotropic accelerations. The basic approach is to analyze equation (19) by visualizing each component of the equation as a geometric object.

The process begins with the torque bounds which are visualized as an n-dimensional hypercube whose center is shifted from the origin by the gravity effect, i.e. $N\mathbf{g}$ from equations (17) and (18). Since the bounds were normalized, equation (13), this hypercube has sides of length 1.

To visualize the isotropic accelerations, we first only consider the end-effector linear acceleration in equation (19);

$$\tau_{lower} \leq E_v\dot{v} \leq \tau_{upper}. \quad (20)$$

The evaluation of the isotropic linear acceleration requires finding the maximum magnitude of $\dot{v}$, that is achievable in every direction. This can be visualized as a hyper-sphere with some radius a,

$$\dot{v}^T\dot{v} = a^2. \quad (21)$$

Since the bounds are represented in torque space, the acceleration hyper-sphere must be mapped into torque space. We have shown [2] that this can be achieved using the following relationships:

$$\tau_v = E_v\dot{v} \quad (22)$$

$$E_v^+\tau_v = \dot{v} \quad (23)$$

where

$$E_v^+ = (E_v^T E_v)^{-1}E_v^T. \quad (24)$$

Using the above relationships, the acceleration hypersphere is transformed into a torque ellipsoid, of dimension three or less of the form,

$$\tau_v^T(E_v E_v^T)^+\tau_v = a^2. \quad (25)$$

This ellipsoid is mapped into the torque bounds. The isotropic acceleration is determined by expanding/contracting the ellipsoid, changing a, until it lies within and is tangent to one of the torque bounds. In Figure 1, this process is shown for a simple case and Figure 2 shows a more general case. The ellipses shown in dashed lines in both figures corresponds to $a = 1$.

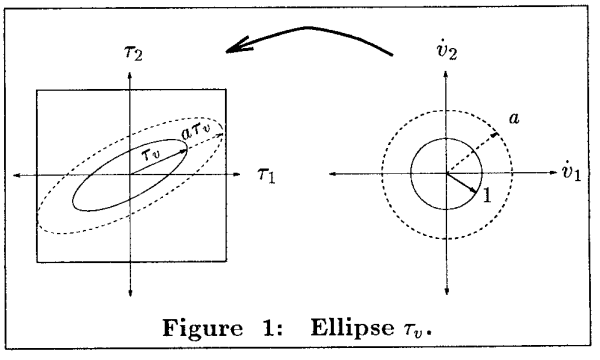

Figure 1: Ellipse τ_v.

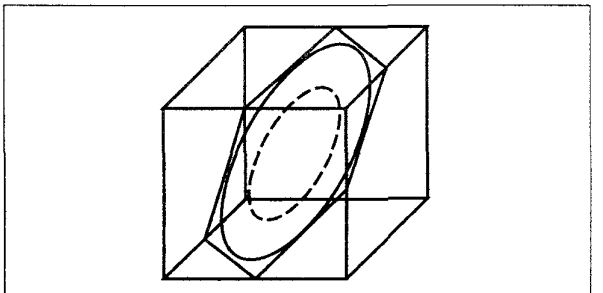

Figure 2: Ellipsoid in 3D.

The same process can be performed on the $E_\omega \dot{\omega}$ term and the resulting ellipsoid is added to the linear acceleration torque ellipsoid within the torque bounds. The centrifugal and Coriolis terms are analyzed by mapping isotropic linear and angular velocity hyper-spheres, $v^T v = c^2$ and $\omega^T \omega = d^2$, through those terms. The information from the resulting surface is then mapped into the torque bounds and added in with the other ellipsoids.

Note that the ellipsoid in equation (25) is completely described by E_v. If the condition number of E_v is equal to one, $\kappa(E_v) = 1$, the ellipsoid is a sphere. Mapping a sphere into the hyper-cube is the best possible situation because an isotropic acceleration capability is achieved while most of the available actuator torque capacity is used. This is true even though the hyper-cube is shifted from the origin by the effect of gravity. The situation improves with the reduction of radius of the hyper-sphere. Then the ellipsoid must be expanded a large amount before reaching the boundaries thus making the isotropic acceleration large.

Also note that this procedure allows to determine the actuator capacity needed to achieve a given desired linear isotropic acceleration. This can be done simply by omitting the normalization of the torque bounds in equation (13). Given a desired isotropic acceleration, a specific value for a, and the equations of motion, the torque ellipsoid in equation (25) is completely determined. The required actuator torques could then be estimated by circumscribing a cube around the ellipsoid. If the overall size of the ellipsoid is made as small as possible, in effect, the required torques to achieve a certain performance will also be minimized.

3.2 Results

The information resulting from the above analysis is in the form of a set of $2n$ inequalities which give the relationship between isotropic end-effector accelerations, $||\dot{v}||$ and $||\dot{\omega}||$, isotropic end-effector velocities, $||v||$ and $||\omega||$, and actuator torque capacity. These equations are used to produce plots of surfaces and curves which describe the relationships between the variables. An example of one of these plots is given in Figure 3 for the PUMA560, where $||\omega|| = 0$.

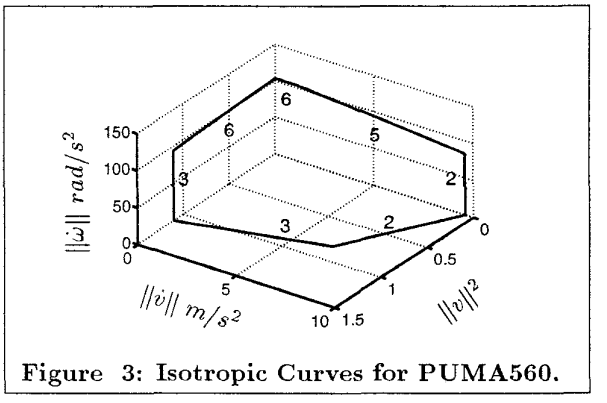

Figure 3: Isotropic Curves for PUMA560.

The above plot should show a three dimensional surface, however only the lines where the surface intersects the coordinate planes are shown. The numbers labeling each line segment represent the actuator whose capacity has been the limiting factor for the accelerations along that line segment.

4 Optimization Scheme

4.1 Cost Function

The cost function should reflect the goals of the optimization as closely as possible. The stated goals can be achieved by minimizing the norms and condition numbers of the mass, inertia, E_v, and E_ω matrices. Towards this end the cost function at a given configuration is defined as;

$$\begin{aligned} cost_i \;=\; & w_1\,\kappa(\Lambda_v) \;+\; w_2\,\kappa(\Lambda_\omega) \;+\; w_3\,||\Lambda_v|| \;+ \\ & w_4\,||\Lambda_\omega|| \;+\; w_5\,\kappa(E_v) \;+\; w_6\,\kappa(E_\omega) \;+ \\ & w_7\,||E_v|| \;+\; w_8\,||E_\omega|| \end{aligned} \tag{26}$$

where w_i is a weight, $\kappa(X)$ is the condition number of X, and $||X||$ is the norm of X.

Optimizing the manipulator's performance over the entire workspace requires consideration of more than one configuration. The properties of the end-effector should change continuously as the manipulator configuration changes. Therefore it is possible to select a representative configuration for a group of nearby or symmetric configurations such that the properties of the group are within some range of this configura-

tion. The optimization over the workspace requires the evaluation of equation (26) over the set of i representative configurations to obtain the total cost;

$$cost = \sum_i cost_i.$$

4.2 Iteration

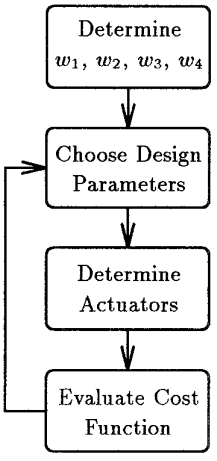

Figure 4: Optimization Flowchart.

The steps in our optimization are shown in Figure 4. The first step is to determine the weights to use in the cost function. Weights are basically determined empirically. The cost function is evaluated at some sample design parameters to determine a range of values for each component. This information can be used to tailor the process to ones particular goals. For instance a rough normalization of each component can be achieved so that each may have the same importance in the cost function. It is important to mention that the final solution is highly dependent on the choice of weights.

An initial estimate at the design parameters is the input to the process. Given the initial design and the desired performance, in terms of desired linear and angular isotropic accelerations at some velocity state, the required actuators can be determined as discussed in section 3.1. A list of possible actuators must be provided as input to the process. The actuators are chosen such that their torque capacity is greater than, yet nearest to, the required torque. However a new selection of actuators alters E_v and E_ω, in turn possibly altering the required torque. Thus some iterations may be needed to obtain convergence between required torques and selected actuators.

Once the actuators have been found, the inertial properties of the manipulator are completely determined and the cost function is evaluated. This value is sent back to the search algorithm which determines the next set of design parameters. Our search has been performed using a steepest descent search algorithm.

5 Application

The mechanism we have chosen is the three-degree-of-freedom parallel mini-manipulator [8] shown in Figure 5. It consists of upper and lower plates connected by three identical ball screws. The ball screws are attached to the fixed lower plate by a one-degree of freedom passive joint, and to the top plate by a three-degree of freedom passive joint. The actuators are mounted to the ends of the ball screws beneath the lower plate.

The manipulator is designed to supply fast motions in one translation and two rotations. Thus we analyze the linear acceleration in the direction perpendicular to the lower plate and the two rotations about the axes in the plane of the lower plate. The isotropic linear acceleration is the acceleration in one direction. The design parameters optimized were the mass of the upper plate and the pitch of the ball screw. Actuators were chosen from a discrete set. The desired performance was specified as, $||\dot{v}|| = 150m/s^2$, $||\dot{\omega}|| = 0m/s^2$, $||v|| = 0m/s$, and $||\omega|| = 0rad/s$ for all configurations.

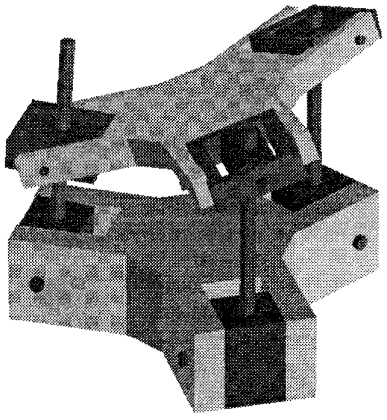

Figure 5: Parallel Mechanism.

The results of the optimization are shown in Table

1 and Figure 6.

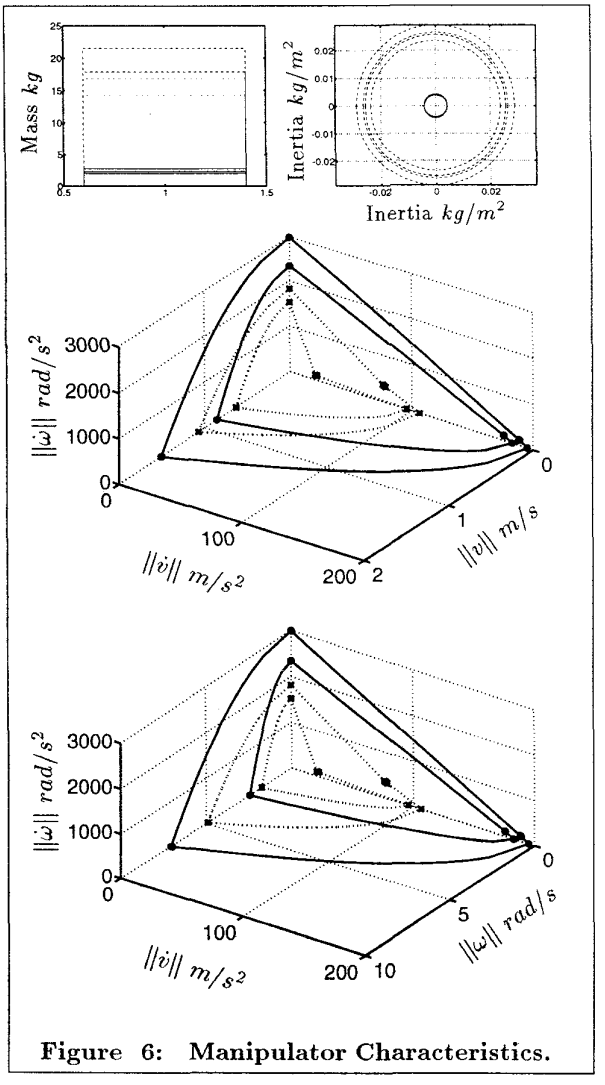

Figure 6: Manipulator Characteristics.

	Initial	Optimized
$\|\|\Lambda_v\|\|$ (kg)	17.5	2.3
$\|\|\Lambda_\omega\|\|$ (kg/m^2)	0.026	0.004
$\|\|E_v\|\|$	2.9×10^{-7}	6.2×10^{-7}
$\|\|E_\omega\|\|$	1.2×10^{-8}	2.9×10^{-8}
$\kappa(\Lambda_v)$	1	1
$\kappa(\Lambda_\omega)$	1.04	1.02
$\kappa(E_v)$	1	1
$\kappa(E_v)$	1.1	1.1

Table 1: Average Properties.

In Figure 6 the inertial and acceleration properties at five different configurations are shown as overlayed bar graphs. The inertia properties are represented as overlayed ellipses. In both graphs the dotted or dashed lines show the initial design and the solid bars show the optimized design. The improvements in these properties is clearly shown and the average values for these properties over the five configurations are given in Table 1.

Below these two graphs are given plots of the isotropic curves; the top plot was generated with $||\omega|| = 0rad/s$ and the lower one with $||v|| = 0m/s$. In both plots the dotted lines indicate the initial design while the solid lines represent the optimized design. In the figure only the maximum and minimum boundaries for the isotropic curves are shown; the isotropic curves for the five configurations lie in the region between the two plotted curves. Its important to underline that the desired performance was exceeded for all configurations. The same actuators were used for the initial and final designs.

The statistics for the initial and optimized designs are given in Table 1. There is improvement in most components of the cost function except $||E_v||$ and $||E_\omega||$. From this it appears that acceleration capability has been sacrificed for better mass properties. However the performance goals where achieved using the same actuators in both designs. This shows the importance of weighting $||E_v||$ and $||E_\omega||$ a little less than the other terms in the cost function to allow the optimization algorithm to find this solution. Determining the weights to achieve the desired characteristics may require several iterations. The initial design parameters were: pitch of ball screw $= 1$ mm/rev and mass of top plate $= 0.7$ kg. The final design parameters were: pitch of ball screw $= 4$ mm/rev and mass of top plate $= 0.5$ kg.

6 Conclusion

In this article we have presented a methodology for the optimization of the dynamic characteristics of manipulators. The formulation is based on our recent studies concerning end-effector inertial and acceleration properties. In particular, the decomposition of these characteristics into two separate models describing linear and angular motions allow more physically meaningful descriptions of these properties. The effectiveness of this methodology has been illustrated in the design of a three-degree-of freedom parallel mini-manipulator system. The process resulted in about a seven fold improvement in the inertial properties while achieving a desired performance level.

Acknowledgments

The financial support of NASA/JPL, Boeing, Hitachi Construction Machinery, and NSF, grant IRI-9320017, are gratefully acknowledged. Many thanks to Professor Bernard Roth and Professor Walter Murray who have made valuable contributions to this work.

References

[1] Asada, H.: Dynamic Analysis and Design of Robot Manipulators Using Inertia Ellipsoids, *Proceedings of the IEEE International Conference on Robotics*, Atlanta, March 1984.

[2] Bowling, A. and Khatib, O.: Analysis of the Acceleration Characteristics of Non-Redundant Manipulators, *Proceedings IEEE/RSJ International Conference on Intelligent Robots and Systems*, Pittsburgh, August 1995.

[3] Hogan, N.: Impedance Control of Industrial Robots, *Robotics Computer-Integrated Manufacturing* vol.1, no. 1, pp. 97-113.

[4] Khatib, O.: Inertial Properties in Robotic Manipulation: An Object-Level Framework, *The International Journal of Robotics Research*, vol. 13, no. 1, February 1995, pp. 19-36.

[5] Khatib, O. and Burdick, J.: Dynamic Optimization in Manipulator Design: The Operational Space Formulation, *The International Journal of Robotics and Automation*, vol.2, no.2, 1987, pp. 90-98.

[6] Khatib, O. and Agrawal, S.: Isotropic and Uniform Inertial and Acceleration Characteristics: Issues in the Design of Redundant Manipulators, *IUTAM/IFAC Symposium on Dynamics of Controlled Mechanical Systems*, Zurich, Switzerland, 1989.

[7] Kim, Y. and Desa, S.: The Definition, Determination, and Characterization of Acceleration Sets for Spatial Manipulators, *The International Journal of Robotics Research*, vol. 12, no. 6, 1993, pp. 572-587.

[8] Waldron, K. J., Raghavan, M. and Roth, B.: Kinematics of a Hybrid Series-Parallel Manipulation System. *Journal of Dynamic Systems, Measurement, and Control*, Vol. 111, pp. 211-221, 1989.

[9] Yoshikawa, T.: Manipulability of Robotic Mechanisms, *The International Journal of Robotics Research*, Vol. 4, No. 2, MIT Press, 1985.

[10] Yoshikawa, T.: Dynamic Manipulability of Robot Manipulators, *Proceedings 1985 IEEE International Conference on Robotics and Automation*, St. Louis, 1985, pp. 1033-1038.